

Long-Term Performance of Borehole Heat Exchanger Fields with Groundwater Movement

S. Lazzari ^{*,1}, A. Priarone ² and E. Zanchini ¹

¹ Dipartimento di Ingegneria Energetica, Nucleare e del Controllo Ambientale
Università di Bologna - Viale Risorgimento 2, I-40136, Bologna, Italy

² Dipartimento DIPTEM - Sezione TEC, Università degli Studi di Genova
Via all'Opera Pia 15A, I-16145, Genova, Italy

*Corresponding author: stefano.lazzari@unibo.it

Abstract: A numerical investigation of the long-term performance of double U-tube borehole heat exchanger (BHE) fields is performed by means of COMSOL Multiphysics, in the case of non-negligible effects of groundwater movement.

Two time periodic heat loads, with a period of one year, are studied: Q_1 , with a partial compensation between winter heating (main load) and summer cooling; Q_2 , with no summer cooling. By assuming a distance of 6 m between adjacent BHEs, the following BHE field configurations are analyzed for a 50-year period: a single line of infinite BHEs; two staggered lines of infinite BHEs; four staggered lines of infinite BHEs. The BHE working fluid is a water-ethylene glycol 20% solution with a minimum allowed temperature equal to -5°C . The ground is modelled as a Darcian porous medium with an undisturbed temperature of 14°C . Three values of the groundwater velocity are investigated: $W = 0$, 10^{-7} and 10^{-6} m/s.

Keywords: Ground Coupled Heat Pumps, Borehole Heat Exchanger (BHE) Fields, Groundwater Movement, Long-Term Operation, Finite Element Simulations.

1. Introduction

Borehole Heat Exchangers (BHEs) allow the heat transfer between the ground and a fluid, typically water or a water-glycol solution. They are generally composed of two U-bent polyethylene vertical tubes, placed in a borehole which is then grouted. The total length of the BHEs necessary for a plant is usually determined by a method recommended by ASHRAE [1].

The correct prediction of the long-term BHE field performance is a crucial problem in designing a BHE installation, especially when no groundwater flow occurs in the ground and the

winter and summer thermal loads are unbalanced. Indeed, either an insufficient distance between BHEs or a too high thermal load per unit length can lead to the system collapse in a few decades.

Few studies on the long-term performance of BHE fields can be found in the literature, and direct experience is lacking, due to the rather recent use of this technology. In Refs. [2, 3] the long-term performance of a coaxial BHE, used only in heating mode for the need of a single family house, is studied. The authors show that the long-term performance of the system stabilizes after the first few years. Moreover, they show that, if the BHE is stopped after a working period of 30 years, the ground temperature reaches approximately the undisturbed initial value after 30 years of recovery. Signorelli et al. [4] simulate the long-term thermal behaviour of an array of six double U-tube BHEs working only in heating mode, and consider an operation period of 30 years. They conclude that, for a BHE array, the recovery time is much longer (70 years).

A more systematic study of the effect of unbalanced winter and summer heat loads on the long-term performance of BHE fields, in the absence of groundwater movement, is presented in Ref. [5]. The authors consider a single BHE, a square field of 4 BHEs and the limiting case of a square field with infinite BHEs, and draw the following conclusions. For a single BHE, no compensation between winter and summer loads is necessary; for a small field of 4 BHEs with a mutual distance of 6 m, a partial compensation of the winter load by means of an opposite-sign summer load with 50% peak power is sufficient to grant an acceptable long-term performance; for a very large and square BHE field, the only solution is an almost complete seasonal compensation of the thermal load.

Clearly, the groundwater movement may soundly improve the long-term performance of

BHE fields. A few studies on the thermal behaviour of BHEs placed in soil with groundwater movement can be found in the literature.

Diao, Li and Fang [6] determine an analytical solution for the time dependent temperature field surrounding a BHE placed in a soil with groundwater movement, under the following simplified scheme: the BHE is treated as a line heat source which releases a uniform and constant power per unit length, starting from the initial instant $\tau = 0$, when the soil has a uniform temperature T_0 . Then, they illustrate the effect of groundwater movement on the temperature field around a single BHE or a set of 6 BHEs subjected to a constant heat load. Fan et al. [7] illustrate the effect of groundwater movement on the performance of a special ground heat exchanger, composed of 37 tubes at a distance of 60 cm from each other, which during winter supplies heat to buildings while, during summer, cools the ground at night and provides air conditioning at daytime. A working period of 15 days is considered for summer, and one of 60 days is considered for winter operation. In Ref. [8] the thermal response of a BHE placed in a ground with relevant water movement is investigated experimentally, both in heating and cooling conditions. Five experimental runs are considered, each performed with a constant water inlet temperature and a duration typical of thermal response tests (30–40 hours). Then, the effect of the groundwater movement on the BHE performance is evaluated by a computational method.

None of these studies focuses on the effects of groundwater movement on the long-term performance of wide BHE fields subjected to unbalanced winter and summer thermal loads.

In the present paper, the long-term performance of double U-tube BHE fields, in the presence of non-negligible effects of groundwater movement, is studied by finite element simulations. The reference case of single BHE surrounded by infinite ground and BHE fields with different geometries are examined: a single line of infinite BHEs, two staggered lines of infinite BHEs, and four staggered lines of infinite BHEs. The distance between adjacent BHEs is assumed equal to 6 m. The groundwater velocity is supposed to be orthogonal to the BHE lines, and three different velocities are considered: 0, 10^{-7} and 10^{-6} m/s. The ground is

modelled as a porous medium with a porosity equal to 0.4 and an effective thermal conductivity equal to 2 W/(m K). Two time periodic heat loads, with a period of one year, are studied: the first has a partial compensation between winter heating (main load) and summer cooling; the second has no summer cooling.

2. Numerical Model

With reference to a water saturated porous soil having an undisturbed ground temperature equal to 14°C, double U-tube BHEs composed of high density polyethylene PE-Xa tubes in which a water-ethylene glycol 20% solution flows, have been studied.

Two time periodic heat loads, with a period of one year, have been considered: Q_1 , with a partial compensation of winter heating by summer cooling, and Q_2 , with no summer load. In both cases, a regular time dependence of the heat load has been assumed; in fact, short period oscillations of the heat load have a negligible influence on the long-term change of a BHE field performance. For both Q_1 and Q_2 , a sinusoidal time dependence of the heat load during winter has been assumed, with a maximum load per BHE unit length equal to 30 W/m. During summer, a sinusoidal time dependence of the heat load with a maximum value of 15 W/m has been assumed for Q_1 , and no heat load for Q_2 , as illustrated in Figure 1. The heat load has been considered as positive if heat is collected by the BHE and supplied to the building, negative in the opposite case.

The equations of the considered heat loads are:

$$Q_1 = \frac{3}{4} A \sin(\omega \tau) + \frac{1}{4} A |\sin(\omega \tau)| \quad (1)$$

$$Q_2 = \frac{1}{2} A \sin(\omega \tau) + \frac{1}{2} A |\sin(\omega \tau)| \quad (2)$$

$$\text{where } \omega = \frac{2\pi}{P} = 1.9924 \cdot 10^{-7} \text{ rad s}^{-1} \quad (3)$$

is the angular frequency, $P = 1 \text{ year} = 31536000 \text{ s}$ is the period, τ is time, $A = 30 \text{ W/m}$ is the amplitude.

Since the temperature distribution along the vertical direction has a negligible influence on long-term BHE performance, the real 3D heat transfer problem has been reduced to a 2D

unsteady model of the BHE cross section, as shown in Figure 2.

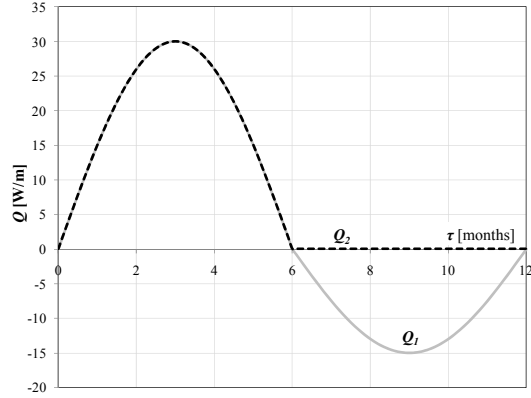


Figure 1. Heat loads Q_1 and Q_2 during one period.

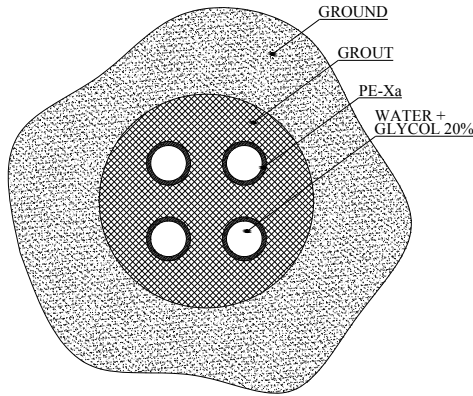


Figure 2. Sketch of the double U-tube BHE cross section.

The long-term simulations of the BHE fields have been performed by considering only the ground as computational domain, with BHEs replaced by holes. The mean temperature of the boundary surface of each hole (interface ground/grout) has been evaluated as

$$T_s(\tau) = \frac{1}{2\pi r_b} \int_S T dl, \quad (4)$$

where r_b is the BHE radius and S is the BHE boundary surface. Then, the mean temperature of the water-ethylene glycol 20% solution, T_f , has been calculated through the BHE thermal resistance per unit length, R_b , as

$$T_f(\tau) = T_s(\tau) + R_b \cdot Q_i(\tau) \quad i = 1, 2 \quad (5)$$

The fluid temperature T_f represents the mean fluid temperature in the BHE, *i.e.*, the arithmetic mean of the inlet and the outlet fluid temperature.

The thermal resistance R_b of the BHE has been evaluated by means of 2D simulations of the steady conduction problem inside the BHE, with the properties of the water-ethylene glycol solution evaluated at two different temperatures: 10°C for the heat load Q_1 , and 6°C for the heat load Q_2 . The physical properties of solid materials have been considered as temperature independent. The values of the BHE geometrical parameters and material properties are summarized in Table 1.

In the evaluation of R_b , the thermal resistance due to the convective heat transfer between the water-glycol and the tube wall has been taken into account by considering an effective thermal conductivity $k_{p\text{eff}}$ of the PE-Xa tube, namely:

$$k_{p\text{eff}} = \frac{\log(r_e/r_i)}{\frac{1}{r_i \cdot h} + \frac{1}{k_p} \cdot \log(r_e/r_i)} \quad (6)$$

where h is the convection coefficient at the internal wall, r_i and r_e are the internal and the external radius of the tube. The values of h have been determined by means of the Churchill correlation [9], for $Re = 3188$ (heat load Q_1) and $Re = 2843$ (heat load Q_2), and are reported in Table 1.

The thermal resistance R_b of the BHE has been evaluated as

$$R_b = \frac{T_i - T_s}{Q} \quad (7)$$

where T_i and T_s are fixed temperatures imposed at the internal wall of each tube and at the external boundary of the BHE, Q is the corresponding heat flux per unit length, which has been determined through a numerical solution of the Laplace equation in a computational domain given by the polyethylene tubes and the grout. The resulting values of R_b are 0.0949 m K/W for the heat load Q_1 (water-glycol solution properties evaluated at 10°C) and 0.1013 m K/W for the heat load Q_2 (water-glycol solution properties evaluated at 6°C).

The accuracy of the approximate method described above, namely the long-term transient

simulation of ground only, and the temperature difference $T_f - T_s$ evaluated through R_b , has been checked by comparing, in one case, the results of the approximate method with those obtained through a complete model, which considers both ground and BHEs in transient computations. An excellent agreement has been found, with a discrepancy in the values of T_f less than 0.05°C .

The long-term performance of double U-tube BHE fields has been studied with reference to the following configurations:

- I - a single BHE surrounded by infinite ground;
- II - a single line of infinite BHEs;
- III - two staggered lines of infinite BHEs;
- IV - four staggered lines of infinite BHEs.

For cases II, III and IV, the distance between two adjacent BHEs has been assumed equal to 6 m. For case I, a square portion of ground with 200 m side has been considered to model the infinite ground around the BHE. Configurations II, III and IV are representative of the working conditions of intermediate BHEs in very long lines.

To study case II, a single BHE has been simulated, centered in a rectangular portion of ground with a length of 200 m and a width equal to 6 m, as sketched in Figure 3a. For case III, a rectangular portion of ground with a length of 200 m and a width equal to 6 m, which contains one BHE and two half BHEs, has been considered (Figure 3b). Similarly, for case IV, a rectangular portion of ground with a length of 200 m and a width of 6 m, which contains two BHEs and four half BHEs has been assumed as the computational domain (Figure 3c).

To model the heat transfer between the BHEs and the ground in presence of groundwater movement, the Darcy model for porous media has been adopted. Thus, the mass, momentum and energy balance equations are

$$\bar{\nabla} \cdot \bar{u} = 0 \quad (8)$$

$$\frac{\mu_w}{K} \bar{u} = -\bar{\nabla} p \quad (9)$$

$$\rho_w c_w \left(\sigma \frac{\partial T}{\partial \tau} + \bar{u} \cdot \bar{\nabla} T \right) = k_{gd\text{ eff}} \nabla^2 T \quad (10)$$

In Eqs. (8)-(10), μ_w , ρ_w , c_w are the viscosity, density and specific heat capacity of the groundwater; K is the permeability [m^2] and ε is the porosity of the medium; the dimensionless parameter σ is defined as

$$\sigma = \frac{\varepsilon \rho_w c_w + (1 - \varepsilon) \rho_{gd} c_{gd}}{\rho_w c_w} \quad (11)$$

and the effective ground thermal conductivity $k_{gd\text{ eff}}$ is given by

$$k_{gd\text{ eff}} = \varepsilon k_w + (1 - \varepsilon) k_{gd} \quad (12)$$

where k_w is the conductivity of groundwater and k_{gd} is that of the solid matrix of the ground.

Table 1. Geometrical parameters and material properties of the BHE.

SYMBOL	VALUE	QUANTITY
Geometrical data of double U-tube BHE		
r_i	13	Internal radius of PE-Xa tube [mm]
r_e	16	External radius of PE-Xa tube [mm]
r_b	78	External radius of grout layer [mm]
Thermal properties of high density polyethylene PE-Xa		
k_p	0.4	Thermal conductivity [$\text{W m}^{-1} \text{K}^{-1}$]
c_p	2300	Specific heat capacity [$\text{J kg}^{-1} \text{K}^{-1}$]
ρ_p	940	Density [kg m^{-3}]
Thermal properties of grout		
k_{gt}	1.5	Thermal conductivity [$\text{W m}^{-1} \text{K}^{-1}$]
$(\rho c)_{gt}$	1.6	Heat cap. per unit vol. [$\text{MJ m}^{-3} \text{K}^{-1}$]
Thermal properties of water-ethylene glycol 20% solution		
$T = 6^\circ\text{C}$		
k_{wg}	0.5036	Thermal conductivity [$\text{W m}^{-1} \text{K}^{-1}$]
c_{wg}	3879	Specific heat capacity [$\text{J kg}^{-1} \text{K}^{-1}$]
ρ_{wg}	1034.2	Density [kg m^{-3}]
μ_{wg}	2.672	Dynamic viscosity [mPa s]
h	198.51	Convection coefficient [$\text{W m}^{-2} \text{K}^{-1}$]
$T = 10^\circ\text{C}$		
k_{wg}	0.5060	Thermal conductivity [$\text{W m}^{-1} \text{K}^{-1}$]
c_{wg}	3885	Specific heat capacity [$\text{J kg}^{-1} \text{K}^{-1}$]
ρ_{wg}	1033	Density [kg m^{-3}]
μ_{wg}	2.380	Dynamic viscosity [mPa s]
h	310.67	Convection coefficient [$\text{W m}^{-2} \text{K}^{-1}$]

Table 2. Properties of ground and groundwater.

SYMBOL	VALUE	QUANTITY
$k_{gd\text{ eff}}$	2	Effective thermal cond. [$\text{W m}^{-1} \text{K}^{-1}$]
$(\rho c)_{gd\text{ eff}}$	2	Eff. heat cap. per unit vol. [$\text{MJ m}^{-3} \text{K}^{-1}$]
ε	0.4	Porosity
k_w	0.58753	Groundwater thermal cond. [$\text{W m}^{-1} \text{K}^{-1}$]
c_w	4189.6	Groundwater spec. heat cap. [$\text{J kg}^{-1} \text{K}^{-1}$]
ρ_w	999.25	Density of groundwater [kg m^{-3}]
W	$0; 10^{-7}; 10^{-6}$	Groundwater undisturbed vel. [m/s]

By introducing the notation $\bar{u} = (u, v)$ and the stream function ψ , one obtains

$$u = \frac{\partial \psi}{\partial y} \quad (13)$$

$$v = -\frac{\partial \psi}{\partial x} \quad (14)$$

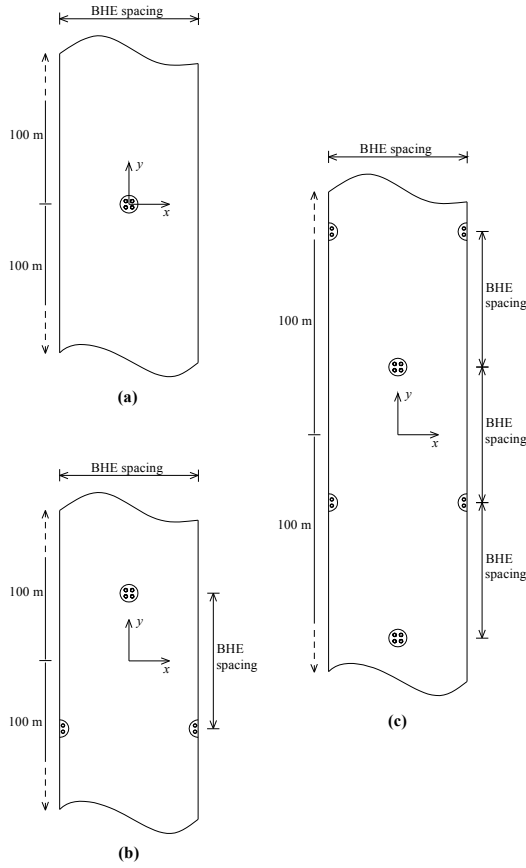


Figure 3. Sketch of the computational domains for lines of infinite BHEs: (a) single line, (b) two staggered lines, (c) four staggered lines.

Then, Eq. (8) is identically satisfied, while Eqs. (9) and (10) become respectively:

$$\nabla^2 \psi = 0 \quad (15)$$

$$\rho_w c_w \left(\sigma \frac{\partial T}{\partial \tau} + \frac{\partial \psi}{\partial y} \frac{\partial T}{\partial x} - \frac{\partial \psi}{\partial x} \frac{\partial T}{\partial y} \right) = k_{gd\,eff} \nabla^2 T \quad (16)$$

The imposed boundary conditions are as follows. At the inlet side of groundwater flow:

$$\frac{\partial \psi}{\partial x} = W, \quad T = T_{gd}, \quad (17)$$

where W is the undisturbed groundwater velocity and T_{gd} is the undisturbed ground temperature.

At the sides parallel to the groundwater flow:

$$\frac{\partial \psi}{\partial y} = 0, \quad \vec{n} \cdot (k_{gd\,eff} \vec{\nabla} T) = 0 \quad (18)$$

At the exit side of groundwater flow:

$$\frac{\partial \psi}{\partial x} = W \quad \text{convective flux} \quad (19)$$

At the interface between ground and BHE (hole)

$$\left(\frac{\partial \psi}{\partial y}, -\frac{\partial \psi}{\partial x} \right) \cdot \vec{n} = 0, \quad (20)$$

$$\vec{n} \cdot (k_{gd\,eff} \vec{\nabla} T) = -\frac{Q_i}{2\pi r_b}, \quad i = 1, 2,$$

where Q_i are the two different time periodic heat loads.

The considered values of groundwater velocity are $W = 0, 10^{-7}$ and 10^{-6} m/s. The initial temperature of the ground is assumed equal to the undisturbed ground temperature, $T_{gd} = 14^\circ\text{C}$, and a volume flow rate of 18 dm^3 per minute in each BHE is considered. The properties of ground and groundwater are reported in Table 2.

For each configuration of the domain, three different meshes have been used for preliminary simulations, performed with $W = 10^{-6}$ m/s. In all the preliminary simulations, the intermediate mesh (Mesh 2) yielded results very close to those obtained by the third, enhanced, mesh. Therefore, Mesh 2 has been adopted for final simulations. This mesh has 3160 triangular elements for the case of a single BHE surrounded by infinite ground, 3610 for the case of a single line of infinite BHEs; it has 3342 elements for the case of two staggered lines of infinite BHEs, and 3376 elements for the case of four staggered lines of infinite BHEs.

3. Results

3.1. Single BHE surrounded by infinite ground

Since the operating fluid is a 20% water-ethylene glycol solution, in the following we will consider acceptable the geometrical configurations and working conditions such that the minimum annual value of T_f remains above -5°C for 50 years.

The time evolution of the mean fluid temperature for a single BHE surrounded by infinite ground, for the heat load Q_2 , is represented in Figure 4, for the groundwater

velocities 0 and 10^{-6} m/s. The figure shows that, for single BHE, the long-term depletion of the BHE performance is not important, even in absence of both heat load compensation and groundwater movement: in this condition, the minimum value of T_f decreases slightly during the first years, then remains practically constant.

The lowest and the highest annual values of T_f for a period of 50 years, for a single BHE in infinite ground, are plotted in Figures 5 and 6, for groundwater velocities equal to 0, 10^{-7} and 10^{-6} m/s. Figure 5 refers to heat load Q_1 and shows that, with this heat load, no appreciable change in time of the lowest and highest annual value of T_f occurs, even for $W = 0$. Figure 6 shows that, for heat load Q_2 , the velocity $W = 10^{-7}$ m/s is sufficient to yield a constant lowest value of T_f after 4 years, while the velocity $W = 10^{-6}$ m/s yields a considerable increase of the lowest value of T_f .

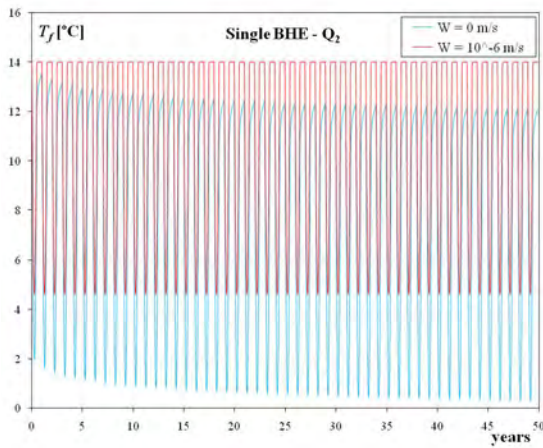


Figure 4. Fluid temperature T_f versus time for a single BHE and heat load Q_2 .

3.2. Single line of infinite BHEs

For a single line of infinite BHEs, plots of the lowest and highest annual values of T_f versus time, for a period of 50 years, are presented in Figures 7 and 8; Figure 7 refers to the heat load Q_1 , while Figure 8 refers to the heat load Q_2 .

As is shown by the figures, in the absence of groundwater movement Q_2 yields the plant collapse, while Q_1 is roughly acceptable. For both heat loads, a groundwater velocity of 10^{-7} m/s is sufficient to stabilize the decrease of the lowest annual value of T_f in a few years, but a velocity of 10^{-6} m/s yields a remarkable increase

of the lowest values of T_f . For heat load Q_2 , it yields also a considerable increase of the highest annual values of T_f , which contributes to the enhancement of the COP of the heat pumps (which work only during winter).

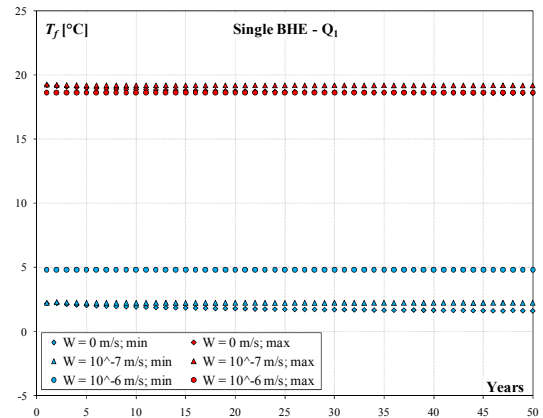


Figure 5. Minimum and maximum annual values of T_f for a single BHE and heat load Q_1 .

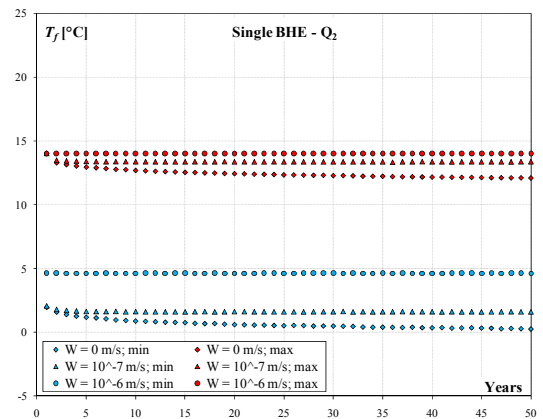


Figure 6. Minimum and maximum annual values of T_f for a single BHE and heat load Q_2 .

Figure 9 shows the temperature field in the ground near a BHE after a working period of about 49 years, for the case of a single line of infinite BHEs, heat load Q_2 , groundwater velocity equal to 10^{-6} m/s. The BHE extracts heat from the ground, which is thus cooled: a thermal wake downstream the BHE is clearly visible and the minimum temperature of the ground is reached at the downstream stagnation point of the BHE wall.

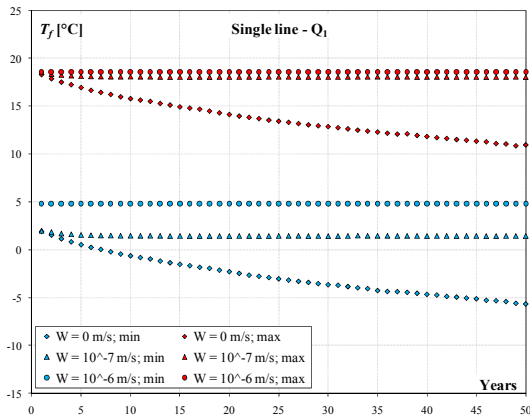


Figure 7. Minimum and maximum annual values of T_f for a single line of BHE and heat load Q_1 .

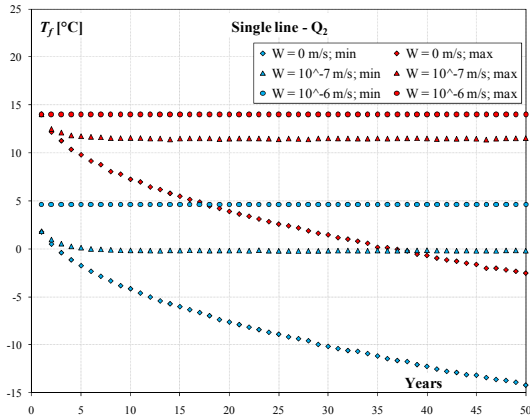


Figure 8. Minimum and maximum annual values of T_f for a single line of BHE and heat load Q_2 .

3.3. Two staggered lines of infinite BHEs

For two staggered lines of infinite BHEs, plots of the lowest and highest annual values of T_f versus time, for a period of 50 years, are presented in Figures 10 and 11; Figure 10 refers to the heat load Q_1 , while Figure 11 refers to the heat load Q_2 . The plotted values of T_f are averaged between the upstream line and the downstream line of BHEs. For this field geometry, both Q_1 and Q_2 are unacceptable in the absence of groundwater movement, while, as in the case of single line, a groundwater velocity of 10^{-7} m/s is sufficient to stabilize the lowest values of T_f after a few years, and to obtain an acceptable situation also for Q_2 . A water velocity of 10^{-6} m/s yields a considerable improvement of the COP of the heat pumps, especially for Q_2 .

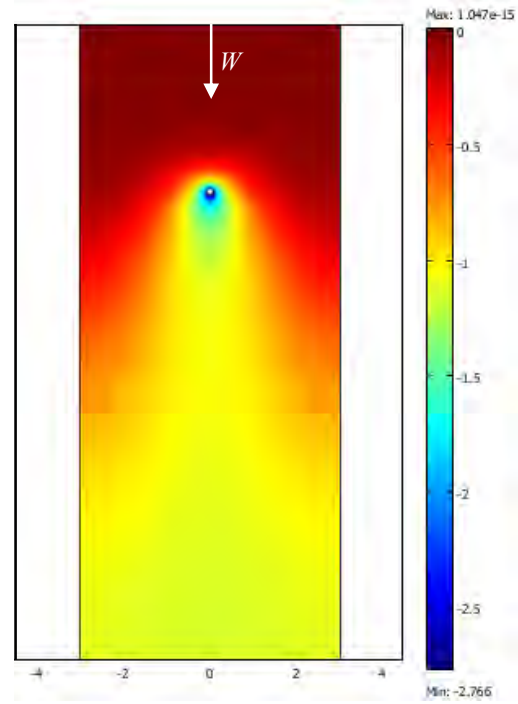


Figure 9. Temperature field in the ground near a BHE: single line, heat load Q_2 , $W = 10^{-6}$ m/s, after 49 years.

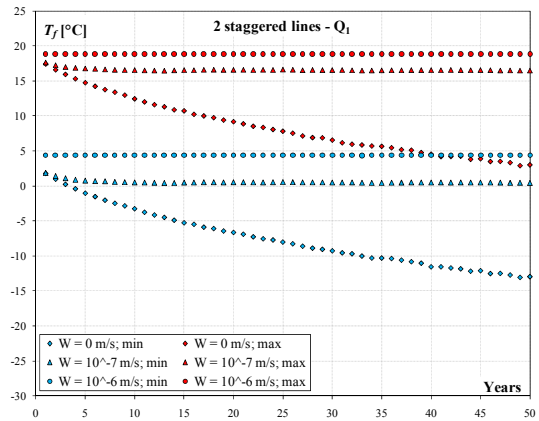


Figure 10. Minimum and maximum annual values of T_f for 2 staggered lines of BHE and heat load Q_1 .

Figure 12 shows the temperature field in the ground after about 49 years, for the case of two staggered lines of infinite BHEs, no compensation heat load Q_2 , groundwater velocity equal to 10^{-6} m/s. The thermal wake produced by the groundwater movement around the upstream BHEs influences the temperature field near the

downstream BHEs which, as a consequence, perform worse than the others.

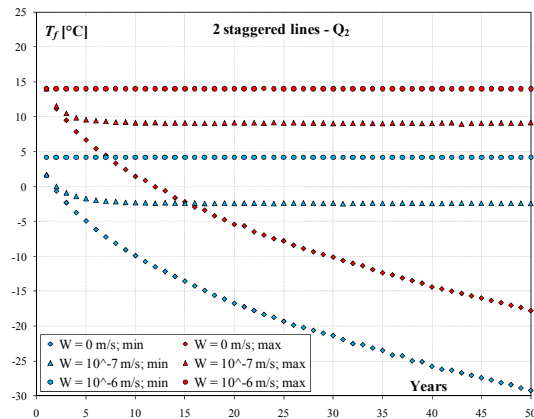


Figure 11. Minimum and maximum annual values of T_f for 2 staggered lines of BHE and heat load Q_2 .

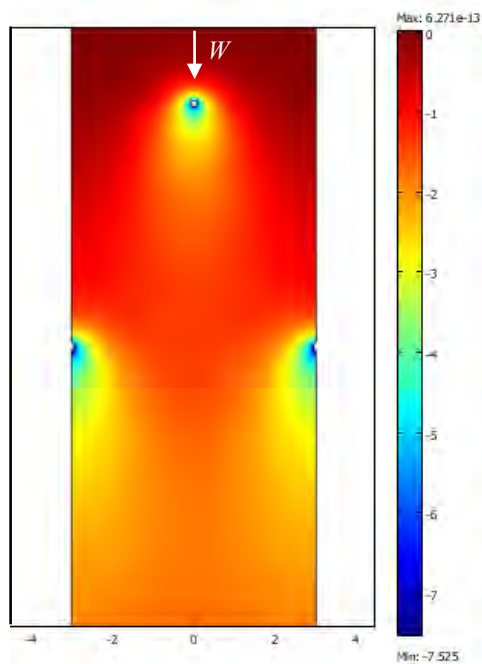


Figure 12. Temperature field in the ground near 3 BHEs: 2 staggered lines, heat load Q_2 , $W = 10^{-6}$ m/s, after 49 years.

3.4. Four staggered lines of infinite BHEs

In the case of four staggered lines of infinite BHEs, plots of the lowest and highest annual values of T_f versus time, for a period of 50 years are presented: Figure 13 refers to heat load Q_1 ,

while Figure 14 to heat load Q_2 . The values of T_f are averaged over the four lines.

For this field geometry, both Q_1 and Q_2 are unacceptable in the absence of groundwater movement. For a groundwater velocity of 10^{-7} m/s, the lowest annual value of T_f becomes constant after 12 years; however, only for Q_1 the lowest temperature reached is acceptable, while Q_2 would require a slightly higher groundwater velocity. A water velocity of 10^{-6} m/s yields acceptable values of T_f for both Q_1 and Q_2 , and ensures a good performance of the ground coupled heat pumps.

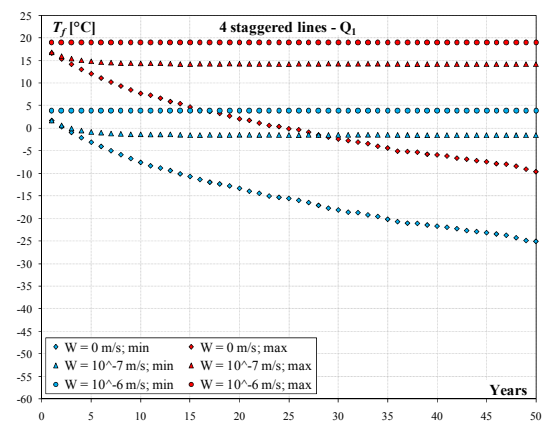


Figure 13. Minimum and maximum annual values of T_f for 4 staggered lines of BHE and heat load Q_1 .

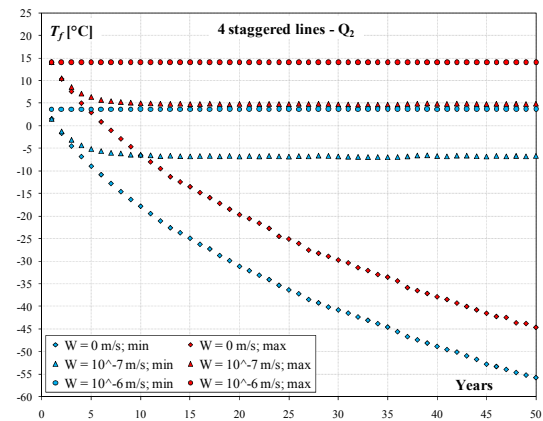


Figure 14. Minimum and maximum annual values of T_f for 4 staggered lines of BHE and heat load Q_2 .

Figure 15 shows the temperature field of the ground after about 49 years, for the case of four staggered lines of infinite BHEs, heat load Q_2 , groundwater velocity equal to 10^{-6} m/s. A

complex interaction among thermal wakes evidences that downstream BHE lines perform gradually worse than upstream lines.

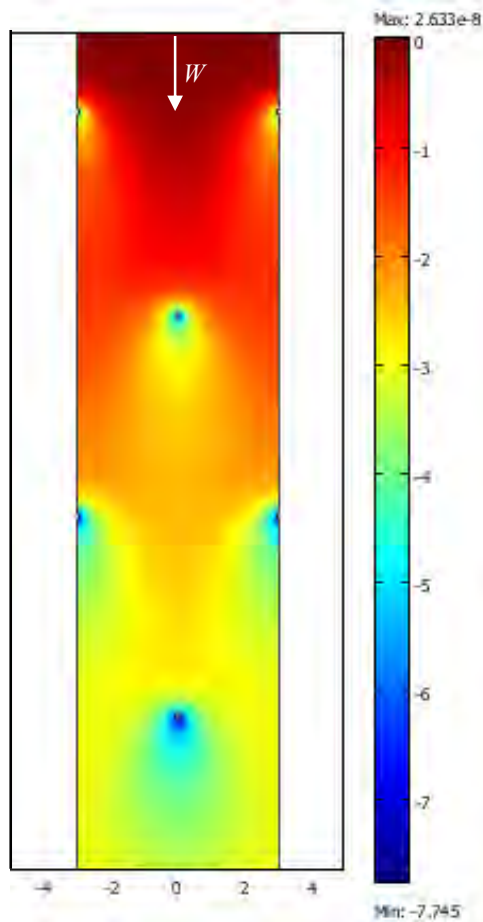


Figure 15. Temperature field in the ground near 6 BHEs: 4 staggered lines, heat load Q_2 , $W = 10^{-6}$ m/s, after 49 years.

4. Conclusions

The long-term performance of double U-tube borehole heat exchanger fields, placed in a porous ground with groundwater movement, has been studied by finite element simulations performed through the software package COMSOL Multiphysics, by considering both a heat load with partial compensation of winter heating with summer cooling and a heat load with no summer cooling. The following results have been obtained, for BHE fields with a distance of 6 m between adjacent BHEs.

For a single BHE surrounded by infinite ground, no compensation between winter and summer loads is needed, even in the absence of groundwater movement. For a single line of infinite BHEs, either a partial compensation of winter and summer loads or some groundwater movement, even very slow, are needed to get an acceptable long-term performance. For two staggered lines of infinite BHEs, a groundwater velocity of 10^{-7} m/s is sufficient to stabilize the lowest annual values of the mean fluid temperature in the BHEs after a few years, and to obtain an acceptable long-term performance, also for winter only operation. For four staggered lines of infinite BHEs, a water velocity of 10^{-7} m/s is sufficient, in the case of partial compensation of winter and summer loads, while a slightly higher velocity is needed in the case of winter only operation. A water velocity of 10^{-6} m/s ensures an excellent long-term performance of the ground coupled heat pumps also in the most critical case examined here, namely that of four staggered lines of infinite BHEs with winter only operation.

5. References

- [1] ASHRAE Handbook -HVAC Appl., Ch. 32 (2007).
- [2] L. Rybach and W.J. Eugster, Sustainability aspects of geothermal heat pumps, *Proc. 27th Workshop on Geothermal Reservoir Engineering*, Stanford University, California, January 28-30, 2002, SGP-TR-171, pp. 1-6.
- [3] L. Rybach, T. Megel, W.J. Eugster, At what time scale are geothermal resources renewable?, *Proc. World Geothermal Congress 2000*, Kyushu - Tohoku, Japan, May 28 - June 10 (2000).
- [4] S. Signorelli, T. Kohl, L. Rybach, Sustainability of Production from Borehole Heat Exchanger Fields, *Proc. World Geothermal Congress 2005*, Antalya, Turkey, 24-29 April.
- [5] A. Priarone, S. Lazzari, E. Zanchini, Numerical Evaluation of Long-Term Performance of Borehole Heat Exchanger Fields, *Proc. COMSOL Conference 2009*, Milan, Italy, 14-16 October.
- [6] N. Diao, Q. Li, Z. Fang, Heat transfer in ground heat exchangers with groundwater

- advection, *Int. Journal of Thermal Sciences*, vol. **43**, pp. 1203-1211, 2004.
- [7] R. Fan, Y. Jiang, Y. Yao, D. Shiming, Z. Ma, A study on the performance of a geothermal heat exchanger under coupled heat conduction and groundwater advection, *Energy*, vol. **32**, pp. 2199–2209, 2007.
- [8] H. Wang, C. Qi, H. Du, J. Gu, Thermal performance of borehole heat exchanger under groundwater flow: A case study from Boading, *Energy and Buildings*, vol. **41**, pp. 1368-1373, 2009.
- [9] S.W. Churchill, Comprehensive correlating equations for heat, mass and momentum transfer in fully developed flow in smooth tubes, *Ind. Eng. Chem. Fundam.*, vol. **16**, pp. 109-116, 1977.